Articles

Optimized Photoisomerization on Gold Nanoparticles Capped by Unsymmetrical Azobenzene Disulfides

Abhijit Manna,[†] Peng-Lei Chen,[‡] Haruhisa Akiyama,[‡] Tian-Xin Wei,[‡] Kaoru Tamada,*[,†,‡] and Wolfgang Knoll[†,§]

Departments of Chemistry and Materials Science, National University of Singapore, Kent Ridge Road, Singapore 17542, Singapore, National Institute of Advanced Industrial Science and Technology (AIST), Tsukuba Center 5, 1-1-1 Higashi, Tsukuba, Ibaraki 305-8565, Japan, and Max Planck Institut für Polymerforschung, Ackermannweg 10, 55128 Mainz, Germany

Received July 18, 2002. Revised Manuscript Received October 22, 2002

Gold nanoparticles capped by an unsymmetrical azobenzene disulfide, 4-hexyl-4′-(12-(dodecyldithio)dodecyloxy)azobenzene (C6AzSSC12), were synthesized in order to investigate the efficiency of azobenzene photoisomerization on colloidal gold surfaces. The nanoparticles were synthesized by a *two-step* method to avoid the direct contact of azobenzene units with a reducing agent. The average size of the particles was determined to be ∼5.2 ± 1.3 nm from transmission electron microscope (TEM) images. The CH_2 antisymmetric (∼2919 cm^{-1}) and symmetric (∼2850 cm^{-1}) stretching bands in the FTIR spectra of the nanocomposite confirmed the all-trans conformation of alkyl chains in the C6AzSSC12 on the colloidal gold. The photoisomerization reaction of the C6AzSSC12-capped gold nanoparticles was studied by UV−vis absorption spectroscopy in toluene. The reaction kinetics was identical to that of the free C6AzSSC12 molecules dissolved in toluene, with no deviations from a first-order plot for both trans-to-cis and cis-to-trans photoisomerization, suggesting no steric hindrance throughout the whole reaction process. The free volume guaranteed by the 50% dilution of the dye functions due to the unsymmetrical disulfide structures, as well as their noncompact molecular tails owing to the assembly on the curved colloidal gold, must be responsible for such a highly efficient photoreaction. Sedimentation of the nanoparticles arose in toluene subsequent to the photoisomerization of the capping azobenzene molecules from trans to cis isomers. This phenomenon can be interpreted as resulting from differences in the degree of solvation between the azobenzene isomers.

1. Introduction

Size-quantized noble metal and semiconductor nanoparticles have drawn considerable interest in various fields of science and engineering because of their unique physical and chemical properties leading to potential applications in electronics, for optical and magnetic devices, in catalysis, as lubricants, and for many other uses.[1,2] Bare nanoparticles are very unstable because of their extremely high surface reactivity. This inherent instability problem of nanoparticles, resulting in their aggregation and subsequent precipitation from the dispersion, has been solved through surface-passivation by self-assembled monolayers (SAMs) of organic molecules (especially alkanethiols and amines).[3,4] By functionalizing SAMs, it is also possible to convey various additional useful properties to the particles, for example, specific packing and self-assembling, special optical and electrical properties, the recognition of chemical and biological molecules, etc.[5−9] There are a few different ways to achieve SAM functionalization, such as using designed multifunctional stabilizers, ligand replacement reactions, and interchain reactions, etc.[10]

* To whom correspondence should be addressed. E-mail: maskt@nus.edu.sg. Tel: +65-6872-0958. Fax: +65-6872-3564.
‡ National Institute of Advanced Industrial Science and Technology.
§ Max Planck Institute für Polymerforschung.
† National University of Singapore.

(1) (a) Faraday, M. *Philos. Trans. R. Soc. London* **1857**, *147*, 145. (b) Turkevich, J. Stevenson, P. C.; Hillier, J. *Discuss. Faraday Soc.* **1951**, *11*, 55. (c) Schmidt, G. *Chem. Rev.* **1992**, *92*, 1709.

(2) (a) Fujihira, M.; Satoh, Y.; Osa, T. *Nature* **1981**, *293*, 206. (b) Henglin, A. *Chem. Rev.* **1989**, *89*, 1861. (c) Freeman, R. G.; Grabar, K. C.; Allison, K. J.; Bright, R. M.; Davis, J. A.; Guthrie, A. P.; Hommer, M. B.; Jackson, M. A.; Smith, P. C.; Walter, D. G.; Natan, M. J. *Science* **1995**, *267*, 1629. (d) Mirkin, C. A.; Letsinger, R. L.; Mucic, R. C.; Storhoff, J. J. *Nature* **1996**, *382*, 607. (e) Elighanian, R.; Storhoff, J. J.; Mucic, R. C.; Letsinger, R. L.; Mirkin, C. A. *Science* **1997**, *277*, 1078. (f) Colvin, V. L.; Schlamp, M. C.; Alivisatos, A. P. *Nature*, **2000**, *407*, 981. (g) Shipway, A. N.; Katz, E.; Willner, I. *ChemPhysChem* **2000**, *1*, 18. (h) Niu, Y.; Yeung, K. L.; Crooks, R. M. *J. Am. Chem. Soc.* **2001**, *123*, 6840.

(3) (a) Brust, M.; Walker, M.; Bethell, D.; Schiffrin, D. J.; Whyman, R. *J. Chem. Soc., Chem. Commun.* **1994**, *801*. (b) Brust, M.; Fink, J.; Bethel, D.; Schiffrin, D. J.; Kiely, C.J *J. Chem. Soc., Chem. Commun.* **1995**, 1655.

10.1021/cm0207696 CCC: $25.00
Published on Web 12/04/2002

Azobenzene-terminated molecules are utilized extensively to introduce dynamic photoresponses on solid surfaces, and recently a few studies have been reported for the synthesis of azobenzene functionalized nanoparticle systems as well.[11,12] However, these studies are mostly using azobenzene-terminated alkanethiolate molecules. These single-chain thiol molecules with aromatic dyes are known to exhibit unique molecular ordering on the planar metal surface due to intermolecular interactions. For example, azobenzene-terminated thiols are known to form densely packed monomolecular films on Au(111) with incommensurate lattices due to nearest-neighbor aggregation.[7] The problem is that such densely packed azobenzene-terminated SAMs are hardly photoreactive upon UV/vis light irradiation.[7d] Referring to the previous reports concerning azobenzene functionalized surfaces[13,14] (such as azosilanes, LB, and thiol-related films) a monomeric dispersion of dye functions with disordered chains seems to be necessary to exhibit high photoreactivity. Actually, it is known that nearest-neighbor aggregation is weaker on the surface of a colloidal gold particle than on a planar gold surface, and even agents with low photoreactivity on planar metal can react on colloidal metals.[11,12,15] On the other hand, these results suggest serious problems with the instability and heterogeneity of the surface for these colloidal systems, as they are strongly due to the curvature of the surface (core size of the particles) or to defects on each metal facet. If we consider future applications with functional nanoparticles, undoubtedly more stable and homogeneous surface reactions will be required.

Scheme 1. Molecular Structure of C6AzSSC12 and Schematic of C6AzSSC12-Capped Gold Nanoparticle

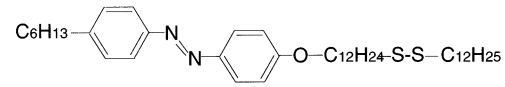

C6AzSSC12

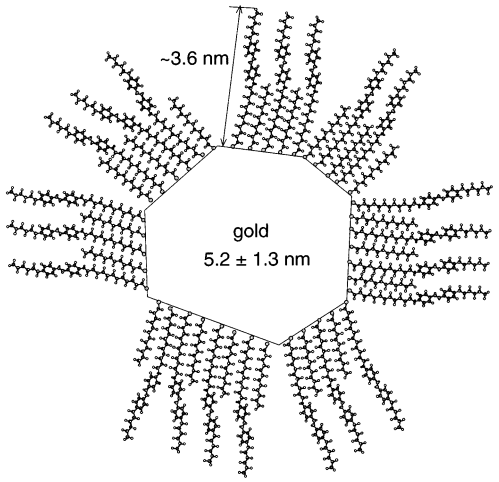

In this paper, we report the synthesis and characterization of gold nanoparticles capped by an unsymmetrical azobenzene disulfide, 4-hexyl-4′-(12-(dodecyldithio)-dodecyloxy)azobenzene (C6AzSSC12, Scheme 1), in an attempt to realize highly efficient photoisomerization on the colloidal gold surfaces. This unsymmetrical azobenzene-disulfide with a short alkyl side chain, C6AzSSC12, was designed in our laboratory originally to realize highly photoreactive SAMs on the planar gold surface.[16−19] In these SAMs, the free volume

(4) (a) Weisbecker, C. S.; Merritt, M. V.; Whitesides, G. M. *Langmuir*, **1996**, *12*, 3763. (b) Manna, A.; Kulkarni, B. D.; Bondoypadhayay, K.; Vijayamohanan, K. *Chem. Mater.* **1997**, *9*, 3032. (c) Hide, F.; Schwartz, B. J.; Diaz-Garcia, M.; Heeger, A. *J. Chem. Phys. Lett.* **1996**, *256*, 424. (d) Balogh, L.; Swanson, D. R.; Spindler, R.; Tomalia, D. A. *Polym. Mater. Sci. Eng.* **1997**, *77*, 118. (e) Zhao, M.; Sun, L.; Crooks, R. M. *J. Am. Chem. Soc.* **1998**, *120*, 4877. (f) Gomez, S.; Erades, L.; Philippot, K.; Chaudret, B.; Colliere, V.; Balmes, O.; Bovin, J−O. *J. Chem. Soc., Chem. Commun.* **2001**, 1474.

(5) (a) Bain, C. D.; Troughton, E. B.; Tao, Y.-T.; Evall, J.; Whitesides, G. M.; Nuzzo, R. G. *J. Am. Chem. Soc.* **1989**, *111*, 321. (b) Hutt, D. A.; Leggett, G. J. *Langmuir* **1997**, *13*, 2740. (c) Sprik, M.; Delamarche, E.; Michel, B.; Röthlisberger, U.; Klein, M. L.; Wolf, H.; Ringsdorf, H. *Langmuir* **1994**, *10*, 4116.

(6) (a) Tamada, K.; Ishida, T.; Knoll, W. Fukushima, H.; Colorado, R., Jr.; Graupe, M.; Shmakova, O. E.; Lee, T. R. *Langmuir* **2001**, *17*, 1913. (b) Frey, S.; Heister, K.; Zharnikov, M.; Grunze, M.; Tamada, K.; Colorado, R., Jr.; Graupe, M.; Shmakova, O. E.; Lee, T. R. *Israel J. Chem.* **2000**, *40*, 81. (c) Alves, C. A.; Porter, M. D. *Langmuir* **1993**, *9*, 3507. (d) Chidsey, C. E. D.; Loiacono, D. N. *Langmuir* **1990**, *6*, 682. (e) Shon, Y. S.; Colorado, R.; Williams, C. T.; Bain, C. D.; Lee, T. R. *Langmuir* **2000**, *16*, 541. (f) Lee, S.; Shon, Y. S.; Colorado, R.; Guenard, R. L.; Lee, T. R.; Perry, S. S. *Langmuir* **2000**, *16*, 2220. (g) Duan, L.; Garrett, S. J. *J. Phys. Chem. B* **2001**, *105*, 9812.

(7) (a) Tamada, K.; Nagasawa, J.; Nakanishi, F.; Abe, K.; Ishida, T.; Hara, M.; Knoll, W. *Langmuir* **1998**, *14*, 3264. (b) Wolf, H.; Ringsdorf, H.; Delamarche, E.; Takami, T.; Kang, H.; Michel, B.; Gerber, Ch.; Jaschke, M.; Butt, H.-J.; Bamberg, E. *J. Phys. Chem.* **1995**, *99*, 7102. (c) Caldwell, W. B.; Campbell, D. J.; Chen, K.; Herr, B. R.; Mirkin, C. A.; Malik, A.; Durbin, M. K.; Dutta, P.; Huang, K. G. *J. Am. Chem. Soc.* **1995**, *117*, 6071. (d) Wang, R.; Iyoda, T.; Jiang, L.; Tryk, D. A.; Hashimoto, K.; Fujishima, J. *Electroanal. Chem.* **1997**, *438*, 213. (e) Shipway, A. N.; Willner, I. *Acc. Chem. Res.* **2001**, *34*, 421.

(8) (a) Revell, D. J.; Chambrier, I.; Cook, M. J.; Russell, D. A. *J. Mater. Chem.* **2000**, *10*, 31. (b) Imahori, H.; Hasobe, T.; Yamada, H.; Nishimura, Y.; Yamazaki, I.; Fukuzumi, S. *Langmuir* **2001**, *17*, 4925. (c) Kondo, T.; Yanagida, M.; Zhang, X. Q.; Uosaki, *Chem Lett.* **2000**, 964.

(9) (a) Neumann, T.; Knoll, W. *Israel J. Chem.* **2001**, *41*, 69. (b) Georgiadis, R.; Peterlinz, K. P.; Peterson, A. W. *J. Am. Chem. Soc.* **2000**, *122*, 3166. (c) Nelson, K. E.; Gamble, L.; Jung, L. S.; Boeckl, M. S.; Naeemi, E.; Golledge, S. L.; Sasaki, T.; Castner, D. G.; Campbell, C. T.; Stayton, P. S. *Langmuir* **2001**, *17*, 2807. (d) Hook, F.; Ray, A.; Norden, B.; Kasemo, B. *Langmuir* **2001**, *17*, 8305. (e) Nyquist, R. M.; Eberhardt, A. S.; Silks, L. A.; Li, Z.; Yang, X.; Swanson, B. I. *Langmuir* **2000**, *16*, 1793. (f) Faull, J. D.; Gupta, V. K. *Langmuir* **2001**, *17*, 1470. (g) Patolsky, F.; Katz, E.; Bardea, A.; Willner, I. *Langmuir* **1999**, *15*, 3703.

(10) (a) Stranick, S. J.; Parikh, A. N.; Tao, Y.-T.; Allara, D. L.; Weiss, P. S. *J. Phys. Chem.* **1994**, *98*, 7636. (b) Schlenoff, J. B.; Li, M.; Ly, H. *J. Am. Chem. Soc.* **1995**, *117*, 12528. (c) Tamada, K.; Hara, M.; Sasabe, H.; Knoll, W. *Langmuir* **1997**, *13*, 1558. (d) Hobara, D.; Sasaki, T.; Imabayashi, S.; Kakiuchi, T. *Langmuir* **1999**, *15*, 5073. (e) Bondoypadhayay, K.; Vijayamohanan, K.; Manna, A.; Kulkarni, B. D. *J. Colloid Interface Sci.* **1998**, *206*, 224. (f) Guyot-Sionnest, P. *Langmuir* **1999**, *15*, 6825. (g) Chung, C.; Lee, M. *J. Electroanal. Chem.* **1999**, *468*, 9. (h) Hostetler, M. J.; Templeton, A. C.; Murray, R. W. *Langmuir* **1999**, *15*, 3782.

(11) Zhang, J.; Whitesell, J. K.; Fox, M. A. *Chem. Mater.* **2001**, *13*, 2323.

(12) Hu, J. H.; Liu, F.; Kittredge, K.; Whitesell, J. K.; Fox, M. A. *J. Am. Chem. Soc.* **2001**, *123*, 1464.

(13) (a) Ichimura, K. *Chem. Rev.* **2000**, *100*, 1873. (b) Sekkat, Z.; Wood, J.; Geerts, Y.; Knoll, W. *Langmuir* **1995**, *11*, 2856; Sekkat, Z.; Wood, J.; Geerts, Y.; Knoll, W. *ibid.* **1996**, *12*, 2976. (c) Xing, L.; Mattice, W. L. *Langmuir* **1996**, *12*, 3024. (d) Siewierski, L. M.; Brittain, W. J.; Petrash, S.; Foster, M. D. *Langmuir* **1996**, *12*, 5838.

(14) (a) Morigaki, K.; Liu, Z.-F.; Hashimoto, K.; Fujishima, A. *J. Phys. Chem.* **1995**, *99*, 14771. (b) Velez, M.; Mukhopadhyay, S.; Muzikante, I.; Matisova, G.; Vieira, S. *Langmuir* **1997**, *13*, 870. (c) Seki, T.; Ichimura, K.; Fukuda, R.; Tanigaki, T.; Tamaki, T. *Macromolecules* **1996**, *29*, 9. (d) Ichimura, K.; Fukushima, N.; Fujimaki, M.; Kawahara, S.; Matuzawa, Y.; Hayashi, Y.; Kudo, K. *Langmuir* **1997**, *13*, 6780.

(15) Evans, S. D.; Johnson, S. R.; Ringsdorf, H.; Williams, L. M.; Wolf, H. *Langmuir* **1998**, *14*, 6436.

(16) Akiyama, H.: Tamada, K.; Nagasawa, J.; Nakanishi, F.; Tamaki, T. *Trans. Mater. Res. Japan* **2000**, *25*, 425.

(17) Tamada, K.; Akiyama, H.; Wei, T. X. *Langmuir* **2002**, *18*, 5339.

(18) Tamada, K.; Akiyama, H.; Wei, T. X.; Kim, S.-A. *Langmuir*, submitted for publication.

for photoreaction of azobenzene moieties is guaranteed by a 50% dilution of dye functions at the outer part of the surface, while a densely packed SAM structure is kept at the bottom of the layer. The photoswitching reaction of C6AzSSC12 SAMs has been well-characterized on planar gold surfaces by means of contact angle measurement, surface-induced liquid crystal (LC) alignment,[16,19] and surface plasmon resonance spectroscopy (SPR).[17,18] As a result, highly efficient photoreactions can be confirmed even on planar gold surfaces because the azobenzene dyes are successfully isolated and dispersed in the SAMs, and only small steric hindrance effects are detected in their reaction kinetics.[17] The photoreaction of the C6AzSSC12 SAM was relatively stable against heat treatment as well, owing to their dense-packed film structures at the bottom composed of dodecanethiolates.[18]

To avoid the reduction of azobenzene groups by contact with $NaBH_4$, we synthesized in this study the capped gold nanoparticles by use of a two-step method, which is different from the conventional synthesis method for alkanethiol-capped nanoparticle developed by Brust et al.[3] Our method consists of the following two steps: step 1, the $NaBH_4$ reduction of extracted $[AuCl_4]^-$ ions into an organic (toluene) phase with tetraoctylammonium bromide (TOAB) as stabilizer; and step 2, the formation of C6AzSSC12 SAMs on the colloidal gold through the surface exchange reaction. The formation of the capped nanoparticles was verified by TEM, FTIR, and UV−vis absorption spectroscopy. The photoisomerization reaction (trans-to-cis and cis-to-trans) of azobenzene dyes on the colloidal gold was characterized by UV−vis absorption spectroscopy in toluene with several intermittent photoirradiations by UV (364 nm) and visible (440 nm) light. The reaction rates were analyzed on the basis of first-order kinetics,[20] and the data were carefully compared to those of the corresponding dye molecules in solution or to those of SAMs adsorbed on planar gold surfaces.[17]

2. Experimental Section

2.1 Reagents. Gold tetrachloro acid trihydrate ($H[AuCl_4]\cdot 3H_2O$, 99%), ethanol (99.8%), toluene (99.8%), sodium borohydride ($NaBH_4$, 96%), tetraoctylammonium bromide (TOAB, 98%), and dichloromethane (100%) were purchased from Merck. All of these chemicals were used without further purification. The unsymmetrical azobenzene disulfide, 4-hexyl-4′-(12-(dodecyldithio)dodecyloxy)azobenzene (C6AzSSC12), was synthesized according to the method reported previously.[16] Milli-Q (MΩcm 18.2 Ω^{1-}) purified water was used throughout all experiments.

2.2 Synthesis of Nanoparticles. The gold nanoparticles were prepared in a two-phase water/TOAB/toluene system. We modified the synthesis method for alkanethiol-capped nanoparticles developed by Brust et al.,[3] to avoid direct contact between the azobenzene group and $NaBH_4$. Our modified method consists of two steps as described in Scheme 2: step 1, the $NaBH_4$ reduction of $[AuCl_4]^-$ ions extracted into an organic (toluene) phase; and step 2, formation of C6AzSSC12 SAMs on the TOAB stabilized nanoparticle surface.

A 30.0 mM $H[AuCl_4]$ aqueous solution (2.5 cm^3) and a 50 mM TOAB toluene solution (7 cm^3) were mixed together and stirred vigorously for ∼20 min. Subsequently, the solution was allowed to separate into two distinct transparent (colorless aqueous and orange-red toluene) phases resulting from a quantitative transfer of Au^{III} ions from the aqueous to the toluene phase. A freshly-prepared 0.2 M $NaBH_4$ aqueous solution (4 cm^3) was slowly added to the two-phase reaction mixture with vigorous stirring. Stirring was continued for 2 h to complete the reaction. The wine-red organic phase was separated and then mixed with a 0.2 M C6AzSSC12 toluene solution (2 cm^3) while stirring. The stirring was continued for 1 h to complete the exchange reaction between C6AzSSC12 and TOAB on the nanoparticle surface. After that, the solution was evaporated at ∼45 °C (at ambient pressure) to reduce the volume to ∼2 cm^3. The concentrated solution was diluted with 100 cm^3 of ethanol and kept in a refrigerator (∼15 °C) for 24 h for precipitation. The precipitate (solid) was extracted and redispersed in 200 mL of a toluene/ethanol (2:3 v/v) mixture by sonication (∼1 min) and reprecipitated. The redispersion and reprecipitation processes were repeated five times in order to remove any free C6AzSSC12 still present in the solid. The purified solid was dried at ∼45 °C at ambient pressure. The yield was 44% with respect to the total weight of Au and C6AzSSC12. The dry powdered nanocomposite obtained could be dissolved to form colloidal solutions in toluene, dichloromethane, and diethyl ether, etc., but it was inert to alkanes. The colloidal toluene solution was stable for months.

Scheme 2. Synthesis of Unsymmetrical Azobenzene Disulfide, 4-Hexyl-4′-(12-(Dodecyldithio)Dodecyloxy)Azobenzene-(C6AzSSC12)-Passivated Au^0 Nanoparticle

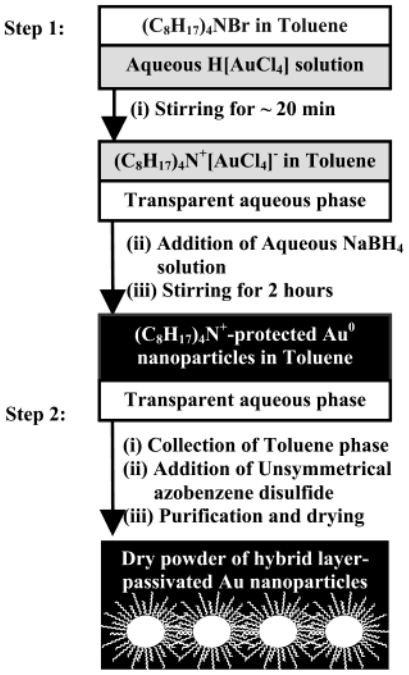

2.3 Characterization. Bright field images of the gold nanoparticles were taken by a transmission electron microscope (TEM; CM 300 FEG Philips TEM operating at 300 kV) at room temperature. Specimens for TEM observation were prepared by spreading a small drop of a dilute colloid solution on a 200-mesh-size copper grid (coated with a Formvar carbon film). The solvent was completely evaporated in air.

Transmission FTIR spectra in the region of 3500−500 cm^{-1} were recorded at 4 cm^{-1} resolution at room temperature on a FTS 135 BIO-RAD FT-IR spectrometer. The specimen was prepared as a KBr pellet of dry composite materials.

UV−visible absorption measurements were carried out at room temperature on a UV-250PC spectrometer (Shimadzu) using a quartz cell (10 mm path). The formation of gold nanoparticles and the photoisomerization reaction of the C6AzSSC12 SAM on the particles were confirmed via absorption of the plasmon band and the spectral change upon photoirradiation, respectively. Toluene was used as the solvent

(19) Akiyama, H.; Tamada, K.; Nagasawa, J.; Abe, K.; Tamada, T. *J. Phys. Chem. B*, in press.
(20) Mita, I.; Horie, K.; Hirao, K. *Macromolecules* **1989**, *22*, 558.

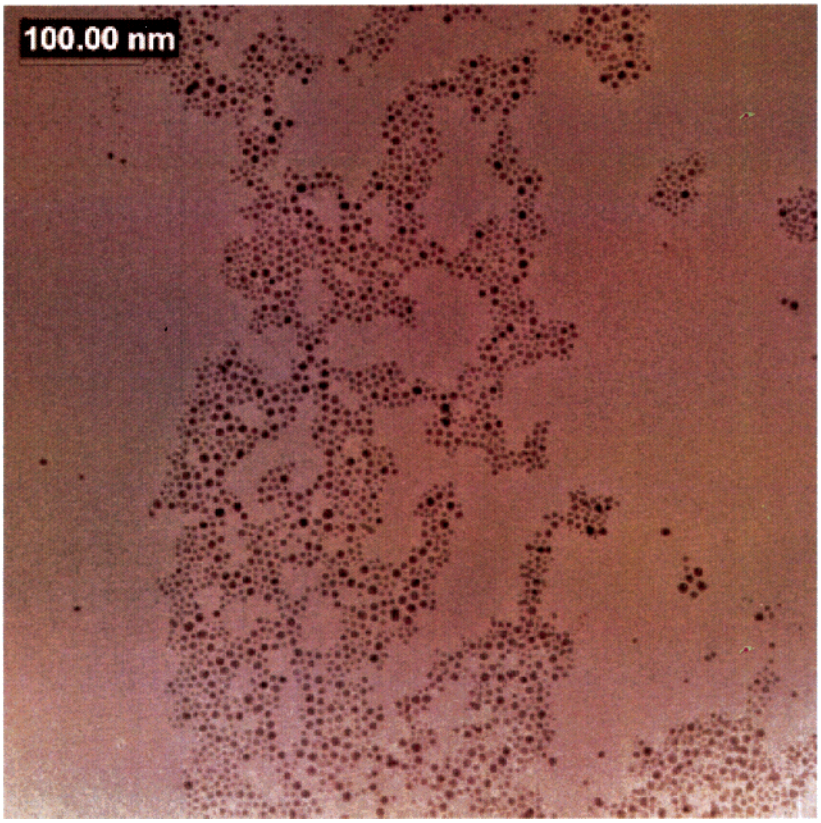

Figure 1. TEM micrograph of C6AzSSC12-capped gold nanoparticles prepared by the two-step method.

for both the C6AzSSC12 molecules and the C6AzSSC12-capped gold nanoparticles,[21] with the concentration of the particle solution (1.4×10^{-2} mg/mL) being controlled to give a peak intensity for the $\pi-\pi^*$ absorption band (λ_{max} ~353 nm) similar to that of the free dye solution (5×10^{-6} M).[22] Photoisomerizations of the free C6AzSSC12 molecules and the C6AzSSC12-capped gold nanoparticles were stimulated upon irradiation with 364- and 440-nm light in liquid cells at room temperature. The light intensities used for the photoisomerization were ca. 1.5 and 0.1 mW/cm^2, respectively. The $\pi-\pi^*$ absorption band (λ_{max} ~353 nm) was used to examine the kinetics of the photoisomerization reaction for both the molecules and the nanoparticles.

3. Results and Discussion

3.1 Particle Size (TEM Images). The size of the C6AzSSC12 gold nanoparticles capped by C6AzSSC12 was examined by TEM. Figure 1 shows a TEM picture of the nanoparticles. All the particles are mostly spherical and two-dimensionally dispersed. The average diameter of the particles is ~5.2 ± 1.3 nm with a distribution range of 2.5−9 nm. As shown in Figure 1, the gold particles form nanostructures onto a Formvar carbon film during the drying process from toluene, where similar-sized particles tend to form more ordered structures with a hexagonal packing. The average edge-to-edge separation between metal cores calculated from the well-ordered region (~3.5 nm) was much shorter than twice the thickness of the C6AzSSC12 SAM ($3.6 \times 2 = 7.2$ nm,[7d] Scheme 1). It is known that the edge-edge spacing between metal cores of alkanethiol-capped nanoparticles is much shorter than twice the molecular length of the alkanethiols utilized, owing to the interdigitation of the alkyl chains between the particles.[23] In a similar manner, the C6AzSSC12 layers on our particles are considered to be interdigitated, as predicted from their molecular structure as shown in Scheme 1.

As discussed, we have prepared the C6AzSSC12 capped gold nanoparticles by a two-step method. In comparison with the particles prepared by the conventional synthesis method for thiol-capped nanoparticles,[2−4] our gold particles are ca. 2 times larger in their size distributions. For our method, the size of the particles is determined at the first reduction process with ammonium ligands (TOAB) as stabilizer. The interaction between gold and the TOAB is not as strong as that between gold and thiols, and apparently the TOAB cannot stabilize tiny particles (<2 nm), unlike the thiol molecules. Originally, we proposed the two-step method to protect the azobenzene units from the reduction. However, because particles with different sizes and a

(21) UV−vis absorption spectrum of the supernatant of C6AzSSC12-capped gold particles in hexane (most particles are precipitated) was measured as well, to confirm that the number of the free dyes in solution was negligibly small.

(22) The number of dye molecules fully adsorbed on one particle is estimated to be ~170 from the average diameter of the particle, $d =$ 5.2 nm (Figure 1), and the cross-section of molecules, 0.50 nm^2/molecule (assumption from lattice constants of azobenzene thiol (5.5 Å) and alkanethiol (5 Å) SAMs). From this value, the number of dyes in the particle dispersion (1.4×10^{-2} mg/mL) is estimated to be 1.5×10^{15} /mL. On the other hand, the number of free dyes in 5×10^{-6} M solution is 3×10^{15}/mL. This good agreement of dye numbers implies (1) the reliability of our measurement, and (2) high molecular density on the gold particles.

(23) (a) Motte, L.; Pileni, M. P. *J. Phys. Chem. B* **1998**, *102*, 4104. (b) Manna, A.; Imae, T.; Iida, M.; Hisamatsu, N. *Langmuir* **2001**, *17*, 6004. (c) Badia, A.; Singh, S.; Demers, L.; Cussia, L.; Brown, R.; Lennox, B. *Chem. Eur. J.* **1996**, *2*, 359.

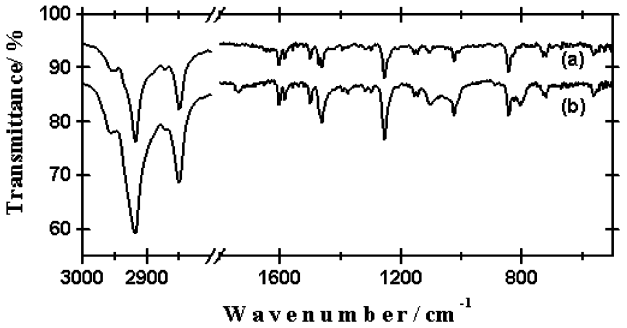

Figure 2. Transmission FT-IR spectra of (a) C6AzSSC12 molecules and (b) C6AzSSC12-capped gold nanoparticles in KBr pellets.

Table 1. FT-IR Bands for Free C6AzSSC12 and C6AzSSC12-Capped Gold Nanoparticles

	band position (*) in cm^{-1}	
assignment	free C6AzSSC12	C6AzSSC12-capped nanoparticles
CH_3 asymmetric stretching	2957 (m)	2957 (m)
	2950 (sh)	
CH_2 antisymmetric stretching	2919 (s)	2919 (s)
CH_3 symmetric stretching	2873 (m)	2873 (m)
CH_2 symmetric stretching	2850 (s)	2850 (s)
benzene C═C skeletal in plane	1604 (m)	1604 (m)
and N═N stretching vibration	1586 (w)	1586 (w)
of azo group	1501 (w)	1500 (m)
CH_2 scissoring of alkyl chain	1472 (m)	1471 (sh)
C═C scalital in plane vibration	1462 (m)	1463 (m)
CH_2 wagging, CH_3 bending	1394 (w)	1394 (w)
(U type), CH_2 twisting, and	1318 (w)	1378 (w)
C−C stretching	1298 (w)	1317 (w)
		1298 (w)
C−O−C asymmetric vibration	1254 (s)	1254 (s)
CH_2 twisting, wagging,	1156 (W)	1156 (w)
and rocking	1146 (w)	1145 (w)
C−O−C symmetric vibration	1105 (w)	1102 (w)
	1025 (w)	1025 (m)
C−C stretching vibration	1008 (sh)	1006 (sh)
	844 m)	840 (s)
CH_2 bending	728 (w)	804 (sh)
	720 (w)	728 (w)
		720 (w)

*Strong (s), medium (m), weak (w), and shoulder (sh).

relatively narrow distribution were obtained consequently, this two-step method can also be considered to be very well suited to control of the size of particles.

3.2 Particle Encapsulation (FT-IR Spectra). Figure 2 shows the transmission FT-IR spectra of C6AzSSC12 molecules and C6AzSSC12-capped gold nanoparticles dispersed in KBr pellets. The characteristic bands of the unsymmetrical azobenzene disulfide are clearly seen in the both cases.[7,19,24,25] The band positions and their assignments are listed in Table 1. The similarity of the two spectra confirms that the unsymmetrical azobenzene disulfide is an essential component of the composite nanoparticles, evidencing the complete exchange of the TOAB layer with the C6AzSSC12 in our two-step synthesis method (no additional peaks related to TOAB were observed in Figure 2b).

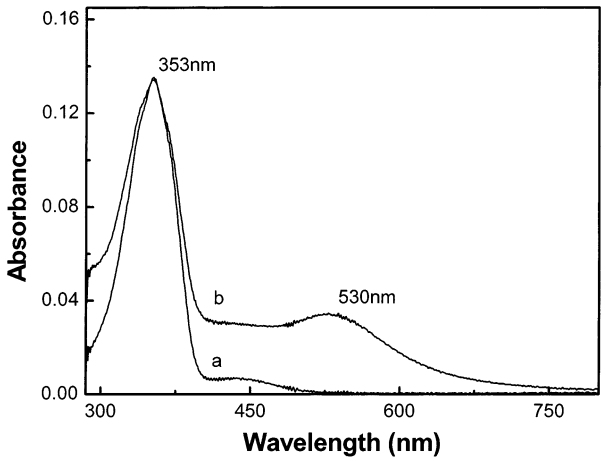

Figure 3. UV−vis absorption spectra of (a) C6AzSSC12 molecules and (b) C6AzSSC12-capped gold nanoparticles (trans form) in toluene.

The peak positions of CH_3 asymmetric ($\nu_{as}(CH_3)$, ∼2957 cm^{-1}) and symmetric ($\nu_s(CH_3)$, ∼2873 cm^{-1}) stretching, CH_2 antisymmetric ($\nu_{as}(CH_2)$, ∼2919 cm^{-1}) and symmetric ($\nu_s(CH_2)$, ∼2850 cm^{-1}) stretching, and CH_2 scissoring modes (∼1472 cm^{-1}) do not change upon the adsorption of the thiols to the nanoparticle surface. These band positions and their invariance suggest that alkyl chains in the C6AzSSC12 molecules exhibit a stretched (trans) conformation for both the adsorbed and the free state.[26] The benzene ring in plane −C═C− (and maybe −N═N−) stretching, the CH_2 wagging, twisting, and rocking, the CH_3 bending, and C−C stretching vibration modes are almost invariant with respect to the adsorption onto the nanoparticle surface. Similar features were observed for C−O−C asymmetric vibration (∼1254 cm^{-1}), whereas C−O−C symmetric vibration (∼1105 cm^{-1}) broadened slightly. In our previous study, we have characterized the infrared reflection absorption (IR-RA) spectra of the C6AzSSC12 SAM on flat Au(111).[19] The peaks attributed to azobenzene moieties were observed at 1603, 1585, 1501, and 1253 cm^{-1} in a manner similar to that for our data in Figure 2. The $\nu_{as}(CH_3)$, $\nu_{as}(CH_2)$, and $\nu_s(CH_2)$ vibrations were observed at around 2967, 2921, and 2851 cm^{-1}, which suggests the trans conformation of alkyl chains with a small portion of gauche structure in the SAM. Evidently, the surface density of the C6AzSSC12 SAM on gold nanoparticles is as high as that of C6AzSSC12 SAM on planar Au(111) or higher. The all trans conformation of the alkyl chains on the nanoparticles must be attributed partially to the densely packed dodecylthiolate layers at the bottom of the SAM but also the terminal hexyl groups interdigitated between the particles in the dry condition as suggested by the TEM image (Figure 1).

3.3 Photoisomerization of Free C6AzSSC12 and C6AzSSC12-Capped Gold Nanoparticles in Toluene (UV−vis Absorption Spectra). Figure 3 shows UV−vis absorption spectra of (a) free C6AzSSC12 molecules and (b) C6AzSSC12-capped gold nanoparticles in toluene. The absorption spectra of the free *trans*-C6AzSSC12 exhibited two clear peaks at the

(24) Dyer, J. R. *Applications of Absorption Spectroscopy of Organic Compounds*, 5th ed.; Prentice-Hall of India: New-Delhi, 1984, p. 22.
(25) Nuzzo, R. G.; Duboli, L. H.; Allara, D. L. *J. Am. Chem. Soc.* **1990**, *112*, 555.
(26) Porter, M. D.; Bright, T. B.; Allara, D. L.; Chidsey, C. E. D. *J. Am. Chem. Soc.* **1987**, *12*, 3559.

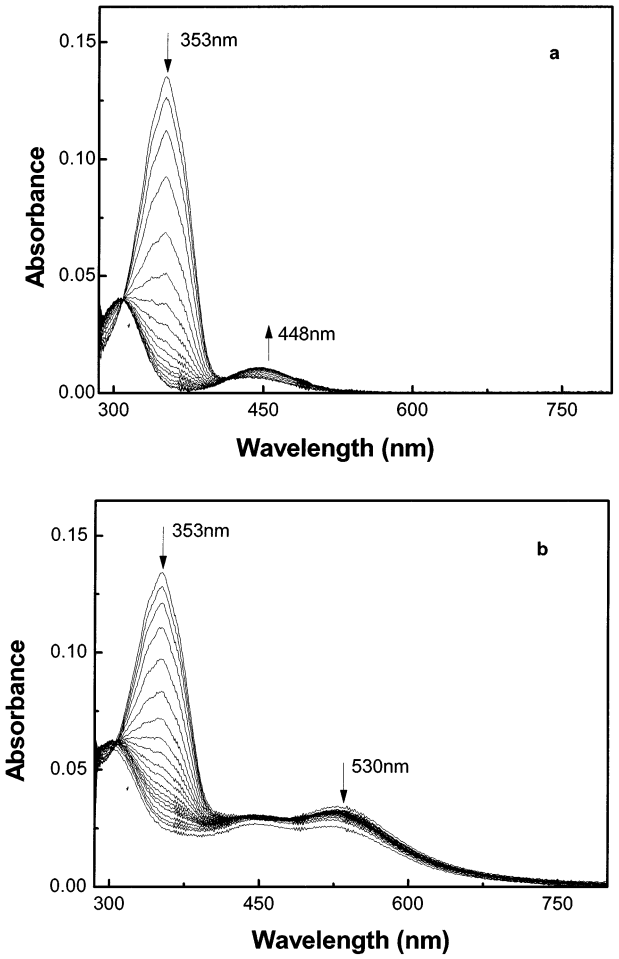

Figure 4. Change in UV−vis absorption spectra of (a) free C6AzSSC12 molecules and (b) C6AzSSC12-capped gold nanoparticles upon intermittent irradiation with UV light (364 nm, $I = 1.5$ mW/cm^2).

wavelengths of ~353 and ~436 nm corresponding to the $\pi-\pi^*$ and $n-\pi^*$ transitions, respectively (Figure 3a).[7a,13] The absorption spectra of the *trans*-C6AzSSC12-capped gold nanoparticles show characteristics similar to those of the free C6AzSSC12 molecules with an additional peak at 530 nm corresponding to a plasmon absorption band (Figure 3b). The appearance of the surface plasmon absorption band is strong evidence for the presence and/or formation of metal nanoparticles in the solution. A comparison between the spectra in Figure 3a and 3b reveals that the $\pi-\pi^*$ absorption at ~353 nm remains invariant toward the passivation of nanoparticle, which proves that the azobenzene dyes are perfectly protected from the reduction during our two-step synthetic method. No shift of the absorption bands also indicates no π-stacking between azobenzene molecules (which may induce a blue shift), and/or no dipole effect on the dyes by being in direct contact with the gold (which may result in a red shift) in our nanoparticle systems.[11,12]

The progress of the photoisomerization reaction of both (a) free C6AzSSC12 molecules and (b) C6AzSSC12-capped gold nanoparticles in toluene is presented in Figure 4. The measurement has been done with intermittent irradiation of UV light (364 nm, $I = 1.5$ mW/cm^2). The result obtained by weaker UV light irradiation ($I = 0.1$ mW/cm^2) is essentially the same, and it is given as Supporting Information. In the case of Figure 4a, the peak intensity at the maximum of the $\pi-\pi^*$ absorption band at 353 nm decreases continuously as the irradiating time increases, with an isosbestic point at ca. 309 nm. For the C6AzSSC12-capped gold nanoparticles in Figure 4b, the intensity of the maximum absorption at 353 nm decreases with the progress of the photoreaction similarly to that shown in Figure 4a; however, the isosbestic point at ca. 309 nm is not as clear as that of the free C6AzSSC12 molecules. The reason is that the whole spectrum of the C6AzSSC12-capped gold nanoparticles, including its plasmon absorption band at ca. 530 nm, decreased distinctly as the photoreaction from the trans to cis isomers progressed. In fact, the last 3 spectra in Figure 4b could be superposed on one another by adjusting the Y range. This phenomenon suggests that the number of gold nanoparticles dispersed in toluene decreased when the azobenzene shell was changed to the cis form. In other words, the particles seem to be precipitating during the isomerization process, as the solubility of *cis*-C6AzSSC12-capped gold nanoparticles is lower than that of the *trans*-C6AzSSC12-capped gold nanoparticles. In fact, the intensities of the plasmon band and the isosbestic point were recovered to the original position by shaking the cell before recording the spectra, though it returned again to the lower value with time. We will discuss the mechanism of the sedimentation of the particles later.

In Figure 5a, we redraw the Figure 4b without the last 3 spectra. All the spectra remaining hold a clear isosbestic point similar to the free C6AzSSC12 molecules in toluene (Figure 4a). By using the data in Figures 4a and 5a, we compared the kinetics of the photoisomerization reaction between the free dye and the dye on the particles. The data were analyzed using a first-order plot based on the equation reported by Mita et al.,[20] where the peak intensities at 353 nm (λ_{max}) are used to determine the progress of the isomerization reaction. The first-order plot obtained is shown in Figure 5b. The reaction of the C6AzSSC12-capped gold nanoparticles shows the identical reaction rate as that of the free C6AzSSC12 molecules, both following first-order kinetics, which suggests no steric effect in the whole reaction process.[27] We investigated the reaction kinetics with the weak light irradiation (364 nm, 0.1 mW) as well. The reaction rate changed in proportion to the light intensity as shown in Figure 6. There is no difference between reaction kinetics for free and the gold-bound species at either of the two intensities investigated.

The cis-to-trans photoisomerization for (a) the free C6AzSSC12 and (b) the C6AzSSC12-capped gold particles in toluene was also examined by irradiation with 440 nm light, and the results are shown in Figure 7. Similar to the trans-to-cis isomerization shown in Figure 4b, the isosbestic point of the C6AzSSC12-capped gold particles is not perfectly clear, and fluctuations of the intensity of the plasmon band and the isosbestic point are observed during the reaction. Probably, the particles precipitated as the cis form and were partly redispersed into toluene during the photoirradiation. Because the

(27) Kinetic data of C6AzSSC12 gold nanoparticles taken by shaking the cells, which kept a clear isosbestic point until the end of reaction, also perfectly agreed with the data shown in Figure 4.

(28) Particles synthesized in our laboratory by the Brust method (ref 3) were utilized for the examination.

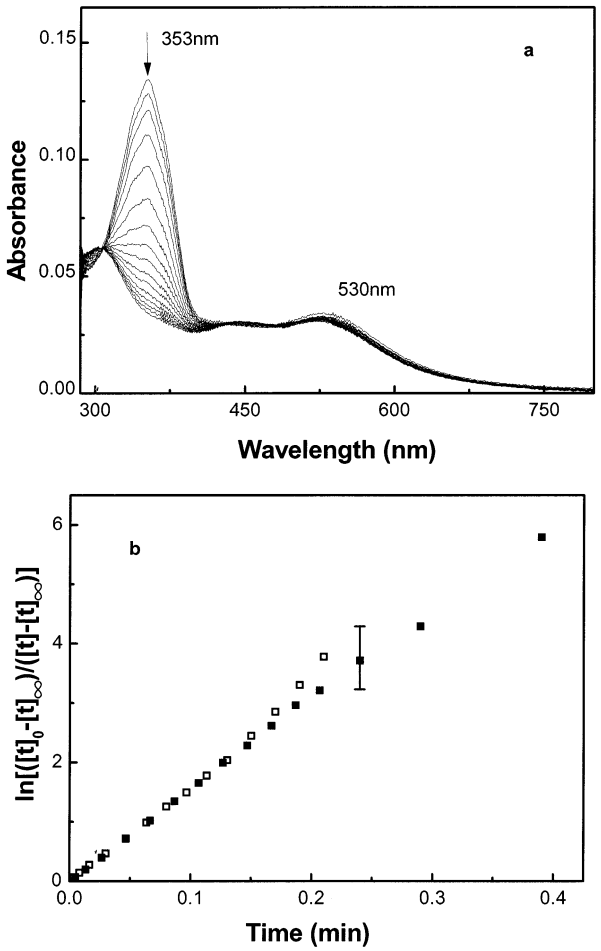

Figure 5. (a) Re-plotted UV−vis absorption spectra of the C6AzSSC12-capped gold nanoparticles by taking out the last 3 spectra from Figure 4b. (b) First-order-plots for trans to cis photoisomerization of free C6AzSSC12 molecule (solid squares) and C6AzSSC12-capped gold nanoparticles (open squares) in toluene determined from the data in Figures 4a and 5a (364 nm, I = 1.5 mW/cm^2). The error in the slope of first-order-plots is ca. ±15% as indicated in the figure.

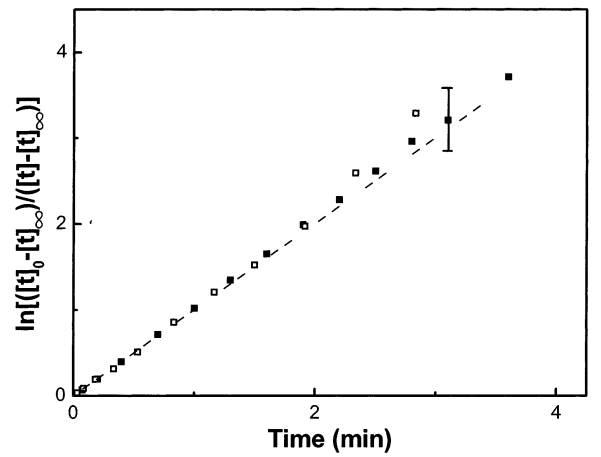

Figure 6. First-order-plots for trans to cis photoisomerization of free C6AzSSC12 molecules (solid squares) and C6AzSSC12-capped gold nanoparticles (open squares) in toluene, upon weak UV light (364 nm, I = 0.1 mW/cm^2) irradiation. The error in the slope of first-order-plots is ca. ±15% as indicated in the figure. The dashed line is the kinetic data of free dye shown in Figure 5b (I = 1.5 mW/cm^2), calibrated by the light intensity.

influence of this fluctuation on the absorbance is much less than that of the trans-to-cis isomerization, we

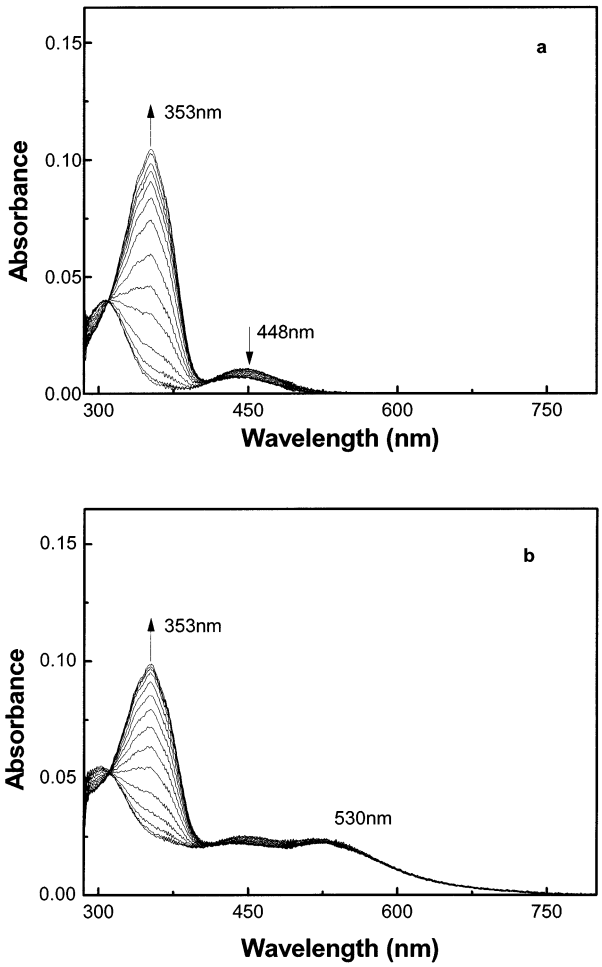

Figure 7. Change in UV−vis absorption spectra of (a) free C6AzSSC12 molecules and (b) C6AzSSC12-capped gold nanoparticles upon intermittent irradiation of vis light (440 nm, I = 1.5 mW/cm^2).

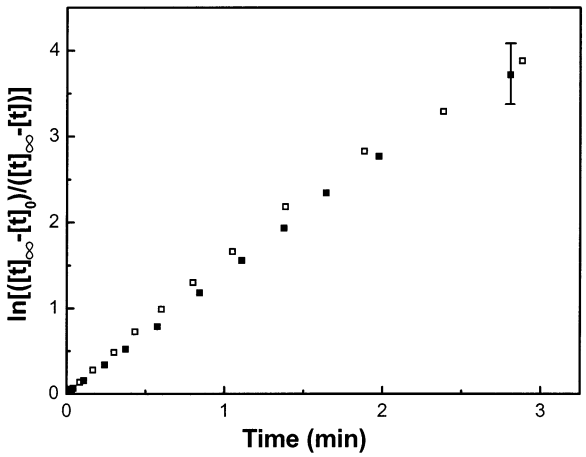

Figure 8. First-order-plots for cis to trans photoisomerization of free C6AzSSC12 molecules (solid squares) and C6AzSSC12-capped gold nanoparticles (open squares) in toluene determined from the data in Figure 7 (440 nm, I = 1.5 mW/cm^2). The error in the slope of first-order-plots is ca. ±15% as indicated in the figure.

conducted the first-order analysis by use of all the spectra in Figure 7, and the result is summarized in Figure 8. As shown in Figure 8, both data exhibited first-order plots with quite similar reaction rates within the error bars, indicating that the cis-to-trans photore-

Scheme 3. Different Degree of "Solvation" Between the Trans- and Cis-C6AzSSC12-Capped Gold Nanoparticles in Toluene

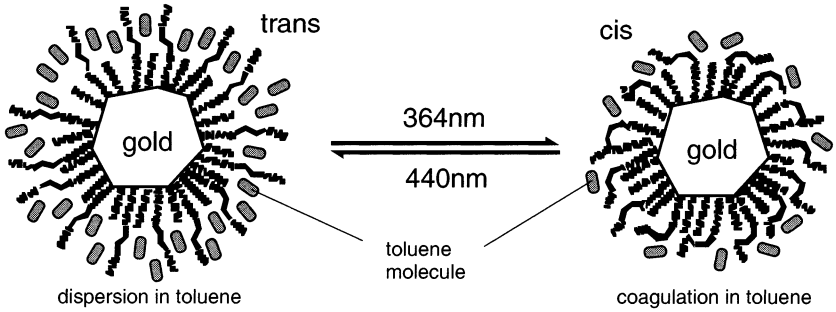

action of the C6AzSSC12-capped gold particles proceeds with a negligible steric effect. The kinetic data with weak light irradiation (440 nm, 0.1 mW) were in good agreement with the data in Figures 7 and 8, and are given as Supporting Information.

It is worth noting that both reactions, the trans-to-cis and the cis-to-trans isomerizations, are free from any steric effect, unlike the reaction on the planar gold surface.[17−18] According to the reaction kinetics of C6AzSSC12 SAM on planar gold determined by SPR measurements, the cis-to-trans photoisomerization almost follows "first-order kinetics", suggesting little steric effect in the reaction process. However, the trans-to-cis photoisomerization exhibits a clear deviation from the first-order plot, indicating a steric effect at the latter part of the reaction. As mentioned in the Introduction, it is known that even molecules with low reactivity on planar gold (e.g., azobenzene-terminated thiol SAMs) can react on colloidal gold, because the curved colloid surface helps to reduce the aggregation and gives free volume for the reaction.[11,12,15] Concerning our C6AzSSC12-capped gold particles, the free volume guaranteed by the 50% dilution of the dye functions due to the unsymmetrical disulfide structure, as well as their non-compact molecular tails assembled on the curved colloidal gold, must work complementarily and enable the ideal reaction on the particles, which is nearly equivalent to the reaction of the free dye molecules in solution.

3.4 Solubility of C6AzSSC12-Capped Gold Nanoparticles in Toluene. The solubility of C6AzSSC12-capped gold nanoparticles is quite different from that of either the free C6AzSSC12 molecules or alkanethiol-capped gold nanoparticles (e.g., with dodecanethiol, C12SH[27]). For example, hexane is a good solvent for the C6AzSSC12 molecules, and was used to prepare the C6AzSSC12 SAMs on planar gold in our previous study.[17,18] Solvation of C6AzSSC12 SAMs with hexane was also clearly confirmed in the SPR data as an increase of film thickness compared with that in air.[17−18] However, the C6AzSSC12-capped gold nanoparticles were hardly dispersed in hexane, whereas the C12SH-capped gold particles could be easily dispersed in hexane. Both the C6AzSSC12 and C12SH SAMs on planar gold are known to exhibit identical contact angles with water, those are a typical value for the SAMs composed of long alkyl chains (C6AzSSC12 SAM θa = 108 ±1°, θr = 94 ±1°;[19] C12SH SAM θa = 108°, θr =99°[29]). In addition, the electric property of the particles determined by the Au−S interface should be common for both particles as well. Thus, the dispersibility of the organic-capped gold nanoparticles in the medium is not yet completely understood and of interest.

The control of dispersibility of colloidal particles by use of their surface reaction with azobenzene derivatives has already been studied by Ueda et al.,[30] though it is a study with relatively large colloidal silica particles (with a diameter of 150 nm). In their study, the calix-[4]resorcinarene with azobenzene functions is adsorbed on the silica surface by hydrogen bonding, however, the density of the azobenzene units was found to be quite low (less than 3%) on the surface.[31] The sedimentation behavior of these silica particles was determined by the decrease in the absorbance at the isosbestic point, and the increase of the surface polarity by the isomerization to the cis form was considered a major reason for the aggregation of the silica particles.

The surface properties of the *trans*- and *cis*-C6AzSSC12 SAMs have been well characterized on planar gold surfaces in our previous studies.[16−19] Dynamic contact angle measurements of C6AzSSC12 SAM against water revealed that the *cis*- C6AzSSC12 SAM has a 4−5 degree lower contact angle than the trans-form SAMs.[19] The lower contact angles of the cis isomer can be interpreted by a larger dipole−dipole interaction between the molecule and the water, as predicted by calculations of the dipole moment of the corresponding dye functions (1.21 D for the trans isomer, and 4.92 D for the cis isomer[19]). We also characterized the "solvation" effect of the C6AzSSC12 SAM for the determination of the optical thickness of the SAMs in our SPR measurements.[17,18] The experimental results revealed that the C6AzSSC12 SAM is highly solvated in *n*-alkanes, unlike the densely packed long-chain thiol (octadecanethiol or azobenzenethiol) SAMs.[17] In addition, the *trans*-C6AzSSC12 SAM is found to be more solvated in *n*-alkanes than the *cis*-C6AzSSC12 SAM (the optical thickness of the *trans*-C6AzSSC12 SAM increased more in contact with *n*-alkanes, compared with that of *cis*-C6AzSSC12 SAM). Following these results, the "free space" in the C6AzSSC12 SAM on the particles, which is also responsible for the interdigitation between

(29) Delamarche, E.; Michel, H.; Kang, H.; Gerber, Ch. *Langmuir* **1994**, *10*, 4103.

(30) Ueda, M.; Fukushima, N.; Kudo, K.; Ichimura, K. *J. Mater. Chem.* **1997**, *7*, 641.

(31) The stability of the self-assembled film on silica was improved by applying another anchoring group (carboxymethylate) to the calix-[4]resorcinarene. (a) Kurita, E.; Fukushima, N.; Fujimaki, M.; Matsuzawa, Y.; Kudo, K.; Ichimura, K. *J. Mater. Chem.* **1998**, *8*, 397. (b) Ichimura, K.; Oh, S. K.; Fujimaki, M.; Mastuzawa, Y.; Nakagawa, M. *J. Inclusion Phenom. Mol. Recognition* **1999**, *35*, 173.

the particles as found in the TEM image (Figure 1), as well as the different polarity of the trans and cis isomers, must provide the different degree of solvation in the azobenzene shells that triggered the change of solubility of the particles (coagulation−dispersion). A schematic model for the solvation of the particles is presented in Scheme 3. We regard this sedimentation of the nanoparticles as additional evidence for the distinguishably high efficiency of the photoreaction in our system.

4. Conclusions

We have synthesized and characterized highly photoreactive gold nanoparticles capped by the unsymmetrical azobenzene disulfide C6AzSSC12. The TEM pictures revealed that our particles have a narrow size distribution with an average diameter of 5.2 ± 1.3 nm, and the edge−edge separation between adjacent metal cores (∼3.5 nm) implied the interdigitation of the C6AzSSC12 shell layers. The all trans conformation of the alkyl chains obtained in the FTIR spectra confirmed the densely packed structure of the C6AzSSC12 SAM on the particles, similar to that on planar gold. Photoisomerizaton reactions of the C6AzSSC12-capped gold nanoparticles were monitored with UV−vis absorption spectroscopy upon irradiation with UV (364 nm) and visible (440 nm) light. The C6AzSSC12-capped gold nanoparticles show reaction rates virtually identical to that of free C6AzSSC12 molecules following first-order kinetics, suggesting no steric effect in the reaction process. The free volume provided by the 50% dilution of dye functions owing to the unsymmetrical disulfide structures, as well as their loosely packed molecular tails owing to the curved colloidal gold surface, is responsible for such an ideal photoreaction. Sedimentation of the C6AzSSC12-capped nanoparticles by photoisomerization from trans to cis isomers was observed in toluene. Different degrees of solvation between trans and cis isomers may trigger the coagulation of the particles. We report this sedimentation of the nanoparticles as evidence of the distinguishably high efficiency of the photoreaction in our nanoparticle system.

Acknowledgment. We thank Prof. A. Huan, Prof. M. Yeadon and Dr. C. S. Yin in IMRE, Singapore, for their kind help with the TEM measurement. We also thank Prof. K. Ichimura in Tokyo University of Science, Japan, for fruitful discussions. This material is based upon work supported by the Science and Engineering Research Council under grants R-152-000-037-303 (A*STAR), and R-152-000-037-112 (MOE). K. Tamada and H. Akiyama acknowledge Dr. K. Yase and Dr. T. Tamaki in AIST for their support in the project of "Harmonized Molecular Materials". Peng-Lei Chen and Tian-Xin Wei thank JST for the JSPS and STA fellowship.

Supporting Information Available: Wavelength graphs of trans to cis photoisomerization and cis to trans photoisomerization, and first-order plots for cis to trans photoisomerization. This material is available free of charge via the Internet at http://pubs.acs.org.

CM0207696